Lattice Boltzmann methods for binary mixtures with different molecular weights

Michael E. McCracken* and John Abraham
Department of Mechanical Engineering, Purdue University, 500 Allison Road, West Lafayette, Indiana 47907, USA
(Received 21 July 2004; published 7 April 2005)

Previous authors have suggested lattice Boltzmann methods for binary mixtures. However, these methods are limited to fluids with nearly the same molecular weight. In this work, two modified methods are proposed for simulating fluids with different molecular weights. The first method is based upon the physical principle that particles with different molecular weights move at different lattice speeds (DLS) when at the same temperature. Therefore, different streaming distances are employed for species with different molecular weights. A second method is developed by selecting constants in the equilibrium distribution function in such a way that the speed of sound can be adjusted for each species. In this approach, the species have the same lattice speed (SLS). Using multiscale expansions, the methods are shown to reproduce the appropriate species continuity equation in the macroscopic limit. The accuracy of the methods is evaluated by studying binary diffusion problems. The DLS method is shown to be able to simulate diffusion in fluids with larger ratios of molecular weights relative to the SLS method.

DOI: 10.1103/PhysRevE.71.046704 PACS number(s): 47.11.+j, 47.10.+g, 05.20.Dd

I. INTRODUCTION

Diffusion among different species is important in many practical applications. These applications include combustion, pollutant dispersion, and chemical reactions. Since the physics of species diffusion on a macroscopic scale is based upon phenomena on a microscopic scale, the lattice Boltzmann method (LBM) is a natural choice for studying these types of problems. Several previous authors have suggested lattice Boltzmann models for binary mixtures [1–4]. The model proposed by Luo and Girimaji [3,4] is firmly based upon kinetic theory. However, their model is limited to fluids with the same molecular weight. In this work, modified models are proposed that allow for simulating fluids with different molecular weights. In the first of the two methods, each species streams with a different lattice speed (DLS) by using different lattice streaming distances while maintaining the same time step. In order to determine the values of the distribution functions at each lattice node, a second-order interpolation scheme is employed. A second method is developed which achieves binary diffusion of fluids with different molecular weights by adjusting constants in the equilibrium distribution function [1]. In this approach, each species has the same lattice speed (SLS), but the speed of sound of each species is adjusted by making the constants in the equilibrium distribution function dependent on the ratio of molecular weights.

In Sec. II, the two binary mixture models are developed by employing the ideas suggested by Luo and Girimaji [3,4]. An interpolation scheme for determining the values of the distribution function for the DLS model is introduced in Sec. III. The methods are shown to reproduce the appropriate species hydrodynamic equations in the macroscopic limit in Sec. IV. In Sec. V, the accuracy of the methods is evaluated by studying binary diffusion problems for species with the same and different molecular weights. The solution for the same molecular weight computation is compared to the solution obtained by employing Fick's law in the macroscopic limit while the solution for the different molecular weight computation is compared to the solution from a computation using a finite difference code with a detailed treatment of multicomponent diffusion. The paper is concluded in Sec. VI.

II. LATTICE BOLTZMANN MODEL FOR BINARY MIXTURES WITH DIFFERENT MOLECULAR WEIGHTS

The lattice Boltzmann method proposed by Luo and Girimaji [4] starts by considering the Boltzmann equation for a binary system,

$$\partial_t f^\sigma + \boldsymbol{\xi} \cdot \nabla f^\sigma + \mathbf{a}_\sigma \cdot \nabla_\xi f^\sigma = Q^{\sigma\sigma} + Q^{\sigma\varsigma}, \tag{1}$$

where f is the probability distribution function, $\boldsymbol{\xi}$ is the particle velocity, σ and ς represent the two species, $\mathbf{a}$ is the acceleration due to a force, $Q^{\sigma\sigma}$ is the self-collision term, and $Q^{\sigma\varsigma}$ is the cross-collision term. In order to convert Eq. (1) into an LBM model, the equation must be integrated in time. The advection terms are integrated along the characteristic directions and the collision terms are integrated using an explicit Euler method. Then the equations are reduced by considering a finite, discrete velocity set. This yields the relationship [4]

$$f_\alpha^\sigma(\mathbf{x} + \mathbf{e}_\alpha \delta_t, t + \delta_t) - f_\alpha^\sigma(\mathbf{x}, t) = J_\alpha^{\sigma\sigma} + J_\alpha^{\sigma\varsigma}\delta_t - F_\alpha^\sigma \delta_t, \tag{2}$$

where

$$J_\alpha^{\sigma\sigma} = -\frac{1}{\tau_\sigma}(f_\alpha^\sigma - f_\alpha^{\sigma(0)}), \tag{3}$$

$$J_\alpha^{\sigma\varsigma} = -\frac{1}{\tau_D}\frac{\rho_\varsigma}{\rho}\frac{f_\alpha^{(0)}}{\delta_t c_s^2}(\mathbf{e}_\alpha - \mathbf{u}_\sigma)\cdot(\mathbf{u}_\sigma - \mathbf{u}_\varsigma), \tag{4}$$

*Corresponding author. Electronic address: michael.e.mccracken@exxonmobil.com

$$F_\alpha^\sigma = -w_\alpha \rho_\sigma \frac{\mathbf{e}_\alpha \cdot \mathbf{a}_\sigma}{c_s^2}. \tag{5}$$

$J_\alpha^{\sigma\sigma}$ and $J_\alpha^{\sigma\varsigma}$ represent the effects due to self-collisions and cross collisions, respectively, while F_α^σ represents the effects due to an external acceleration force, $\mathbf{a}_\sigma$, and α is the velocity direction. The weighting function, w_α, depends on the discrete velocity set $\mathbf{e}_\alpha$. In this work, we will not focus on the effects of a forcing term such as F_α^σ. Other authors have performed more in-depth analyses of forcing terms [5,6]. The cross-collision term given by Eq. (4) is proportional to the difference in the species' velocities, which is equivalent to the difference in the species' diffusion velocities. This is reasonable because the larger the velocity difference, the larger the influence of cross collisions on the equilibrium distribution function. The equilibrium distribution function, $f_\alpha^{\sigma(0)}$, is given by the following equations:

$$f_\alpha^{\sigma(0)} = \left[1 + \frac{1}{c_s^2}(\mathbf{e}_\alpha - \mathbf{u}) \cdot (\mathbf{u}_\sigma - \mathbf{u})\right] f_\alpha^{\sigma(eq)}, \tag{6}$$

$$f_\alpha^{\sigma(eq)} = w_\alpha \rho_\sigma \left[1 + \frac{\mathbf{e}_\alpha \cdot \mathbf{u}}{c_s^2} + \frac{(\mathbf{e}_\alpha \cdot \mathbf{u})^2}{2c_s^4} - \frac{\mathbf{u} \cdot \mathbf{u}}{2c_s^2}\right]. \tag{7}$$

For the D2Q9 model $\mathbf{e}_\alpha$ and w_α are given by

$$e_\alpha = \begin{cases} (0,0), & \alpha = 0 \\ \left(\cos\left[\dfrac{(\alpha-1)\pi}{2}\right], \sin\left[\dfrac{(\alpha-1)\pi}{2}\right]\right) c, & \alpha = 1-4 \\ \sqrt{2}\left(\cos\left[\dfrac{(\alpha-5)\pi}{2} + \dfrac{\pi}{4}\right], \sin\left[\dfrac{(\alpha-5)\pi}{2} + \dfrac{\pi}{4}\right]\right) c, & \alpha = 5-8, \end{cases} \tag{8}$$

and

$$w_\alpha = \begin{cases} 4/9, & \alpha = 0 \\ 1/9, & \alpha = 1-4 \\ 1/36, & \alpha = 5-8, \end{cases} \tag{9}$$

where the lattice speed, c, is related to the lattice spacing by $c = \delta_x / \delta_t$. The macroscopic variables for each species are found from the moments of the distribution functions, i.e.,

$$\rho_\sigma = \sum_\alpha f_\alpha^\sigma = \sum_\alpha f_\alpha^{\sigma(0)}, \tag{10}$$

$$\rho_\sigma \mathbf{u}_\sigma = \sum_\alpha f_\alpha^\sigma \mathbf{e}_\alpha = \sum_\alpha f_\alpha^{\sigma(0)} \mathbf{e}_\alpha. \tag{11}$$

The species' velocities are the sum of the bulk velocity and the species' diffusion velocity, i.e.,

$$\mathbf{u}_\sigma = \mathbf{u} + \mathbf{u}_{\sigma,diff}. \tag{12}$$

The total mass density and mass averaged velocity of the mixture are

$$\rho = \rho_\sigma + \rho_\varsigma, \tag{13}$$

$$\rho \mathbf{u} = \rho_\sigma \mathbf{u}_\sigma + \rho_\varsigma \mathbf{u}_\varsigma. \tag{14}$$

The model presented above is firmly based upon kinetic theory [7,8]. However, the model above cannot simulate binary diffusion of fluids with different molecular weights because the pressure in this model is given by

$$p = (\rho_\sigma + \rho_\varsigma) c_s^2, \tag{15}$$

where $c_s^2 = c^2/3$. This states that the total pressure is equal to the sum of the partial pressures. The derivation of the momentum equation in Sec. IV will show how this expression enters the equation. From Eq. (15), it can be seen that in order for the pressure to be constant the sum of the two species' densities must be constant at every location, but this requirement is not necessary for two species of different molecular weights. In order to deal with this problem, some authors [1] have suggested adjusting the fraction of particles at rest for each species. We will first develop a model for binary diffusion following this suggestion, show its limitations, and then develop another model that is more physically intuitive. In the introduction to this paper, we refer to the former as the SLS method and the latter as the DLS method.

In the SLS method, we alter the speed of sound for each species while maintaining the same lattice speed, c. This approach is not consistent with the *a priori* derivation of the lattice Boltzmann equation from the continuous Boltzmann equation given in Ref. [9], but will provide the correct hydrodynamic equations in the macroscopic limit if done properly. Wolf-Gladrow [10], in chapter 5 of his text, suggests using the following generic form of the D2Q9 equilibrium distribution function in order to have maximum control over the choice of constants, A_0^σ, A_1^σ, A_2^σ, B_1^σ, B_2^σ, C_1^σ, C_2^σ, D_0^σ, D_1^σ, and D_2^σ:

$$f_\alpha^{\sigma(eq)} = \begin{cases} \rho_\sigma(A_0^\sigma + D_0^\sigma \mathbf{u}\cdot\mathbf{u}), & \alpha = 0 \\ \rho_\sigma(A_1^\sigma + B_1^\sigma \mathbf{e}_\alpha\cdot\mathbf{u} + C_1^\sigma(\mathbf{e}_\alpha\cdot\mathbf{u})^2 + D_1^\sigma \mathbf{u}\cdot\mathbf{u}), & \alpha = 1-4 \\ \rho_\sigma(A_2^\sigma + B_2^\sigma \mathbf{e}_\alpha\cdot\mathbf{u} + C_2^\sigma(\mathbf{e}_\alpha\cdot\mathbf{u})^2 + D_2^\sigma \mathbf{u}\cdot\mathbf{u}), & \alpha = 5-8. \end{cases} \tag{16}$$

The constants must be chosen so that mass and momentum are conserved and in such a way as to obtain the proper momentum flux tensor, $P_{ij}^{\sigma(0)} = \Sigma_\alpha e_{\alpha i} e_{\alpha j} f_\alpha^{\sigma(eq)}$, which influences the macroscopic conservation of momentum equation. Following the derivation in Ref. [10] in order to obtain the proper momentum flux tensor, $4C_2^\sigma c^2 + 2D_1^\sigma + 4D_2^\sigma = 0$, $C_1^\sigma = 1/2c^4$, and $C_2^\sigma = 1/8c^4$. Following Ref. [10], we choose to restrict the constants so that

$$\frac{A_0^\sigma}{A_1^\sigma} = \frac{A_1^\sigma}{A_2^\sigma} = \frac{B_1^\sigma}{B_2^\sigma} = \frac{D_0^\sigma}{D_1^\sigma} = r^\sigma. \tag{17}$$

When including the additional requirement that the macroscopic moments are conserved, the following relationships are obtained:

$$A_0^\sigma = \frac{r^{\sigma 2}}{(r^\sigma + 2)^2}, \quad A_1^\sigma = \frac{r^\sigma}{(r^\sigma + 2)^2}, \quad A_2^\sigma = \frac{1}{(r^\sigma + 2)^2}, \tag{18}$$

$$B_1^\sigma = \frac{r^\sigma}{4 + 2r^\sigma}\frac{1}{c^2}, \quad B_2^\sigma = \frac{1}{4 + 2r^\sigma}\frac{1}{c^2}, \tag{19}$$

$$D_0^\sigma = -\frac{r^\sigma}{2 + r^\sigma}\frac{1}{c^2}, \quad D_1^\sigma = -\frac{1}{2 + r^\sigma}\frac{1}{c^2}, \quad D_2^\sigma = -\frac{r^\sigma - 2}{16 + 8r^\sigma}\frac{1}{c^2}. \tag{20}$$

Now the speed of sound for two species can differ by selecting different r^σ from the relationship

$$c_s^\sigma = \sqrt{\frac{2}{r^\sigma + 2}}c. \tag{21}$$

In this approach, Eq. (16) replaces Eq. (7), and the speed of sound in Eq. (6) is now dependent on the species. The pressure in this model follows the equation of state,

$$p = \rho_\sigma c_s^{\sigma 2} + \rho_\varsigma c_s^{\varsigma 2}. \tag{22}$$

In order to eliminate pressure gradients due to concentration differences, the speeds of sound should be selected so that

$$c_s^\varsigma = \sqrt{\frac{m_\sigma}{m_\varsigma}}c_s^\sigma, \tag{23}$$

where m_σ is the molecular mass of species σ. It is important to note that the speed of sound of either species, c_s^σ, cannot exceed the lattice speed, c. In our simulations, we have noticed that as c_s^σ approaches c the computations are numerically less stable. If the slower speed of sound is selected to be $c_s^\sigma = c/\sqrt{3}$ when $m_\sigma > m_\varsigma$, then the maximum density ratio between the species is 3. Lower values of c_s^σ can be employed. However, these values then limit the maximum numerically stable velocity, $|\mathbf{u}|$, due to the low Mach number criteria of the LBM.

In light of these limitations, we propose an alternative physically intuitive approach (referred to as the DLS method earlier) to solve the binary diffusion problem by allowing each species to move with different lattice speeds, c^σ. This will give each species a different speed of sound, $c_s^\sigma = c^\sigma/3$, while still employing a standard equilibrium distribution function that follows the *a priori* derivation [9]. The simplest way to allow for two lattice speeds is to have two different streaming distances and keep the same time step, i.e., $c^\sigma = \delta_x/\delta_t$ and $c^\varsigma = \sqrt{m_\sigma/m_\varsigma}\delta_x/\delta_t$, where the molecular mass of species σ is the larger of the two species. Species σ has a streaming distance of δ_x, and species ς has a streaming distance of $\sqrt{m_\sigma/m_\varsigma}\delta_x$. The problem of completing the streaming step for computations with two different streaming distances will be addressed in the next section. The two different streaming distances lead to a velocity set dependent on species, i.e.,

$$\mathbf{e}_\alpha^\sigma = \begin{cases} (0,0), & \alpha = 0 \\ \left(\cos\left[\frac{(\alpha-1)\pi}{2}\right], \sin\left[\frac{(\alpha-1)\pi}{2}\right]\right)c^\sigma, & \alpha = 1-4 \\ \sqrt{2}\left(\cos\left[\frac{(\alpha-5)\pi}{2} + \frac{\pi}{4}\right], \sin\left[\frac{(\alpha-5)\pi}{2} + \frac{\pi}{4}\right]\right)c^\sigma, & \alpha = 5-8. \end{cases} \tag{24}$$

Now Eqs. (6) and (7) can be written for the modified model as

$$f_\alpha^{\sigma(0)} = \left[1 + \frac{1}{c_s^{\sigma 2}}(\mathbf{e}_\alpha^\sigma - \mathbf{u}) \cdot (\mathbf{u}_\sigma - \mathbf{u})\right] f_\alpha^{\sigma(eq)}, \tag{25}$$

$$f_\alpha^{\sigma(eq)} = w_\alpha \rho_\sigma \left[1 + \frac{\mathbf{e}_\alpha^\sigma \cdot \mathbf{u}}{c_s^{\sigma 2}} + \frac{(\mathbf{e}_\alpha^\sigma \cdot \mathbf{u})^2}{2c_s^{\sigma 4}} - \frac{\mathbf{u} \cdot \mathbf{u}}{2c_s^{\sigma 2}}\right]. \tag{26}$$

Similarly, Eqs. (2), (4), (5), and (11) can be rewritten to account for multiple streaming distances by replacing $\mathbf{e}_\alpha$ with $\mathbf{e}_\alpha^\sigma$. The equation of state for this model can be easily shown to have the following form:

$$p = \rho_\sigma c_s^{\sigma 2} + \rho_\varsigma c_s^{\varsigma 2} = \frac{1}{3}\left(\rho_\sigma + \frac{m_\sigma}{m_\varsigma}\rho_\varsigma\right)\left(\frac{\delta x}{\delta t}\right)^2. \tag{27}$$

This approach is physically consistent because particles with larger molecular weights move at slower speeds relative to lighter particles. Hence, their speeds of sound scale accordingly.

III. SOLVING FOR DIFFERENT STREAMING VELOCITIES

In this section, we propose a scheme for solving the lattice Boltzmann equations with different streaming distances for each species. We use a lattice structure with a distance of $\sqrt{m_\sigma/m_\varsigma}\delta_x$ between lattice nodes where $\sqrt{m_\sigma/m_\varsigma} \geqslant 1$. With this arrangement, the distribution function of species ς streams exactly to its neighboring lattice nodes in one time step. However, the distribution function of species σ will stream to some location between the node of its origin and the neighboring lattice node. In order to determine the values of the distribution function for species σ after the streaming step at each lattice node, a second-order interpolation scheme is employed. Previous authors [11] have suggested using interpolation schemes for implementing nonuniform lattice spacing. We select a second-order Lagrangian interpolation polynomial with the following form:

$$f_\alpha^\sigma(x) = \frac{(x-b)(x-c)}{(a-b)(a-c)} f_\alpha^\sigma(a) + \frac{(x-a)(x-c)}{(b-a)(b-c)} f_\alpha^\sigma(b) + \frac{(x-a)(x-b)}{(c-a)(c-b)} f_\alpha^\sigma(c), \tag{28}$$

where a is the x location of the particle in consideration, i.e., the particle starting at (x,y), after the streaming step, b is the x location of the neighboring particle, i.e., the particle starting at $(x-\sqrt{m_\sigma/m_\varsigma}\delta_t, y)$ for $\alpha=1$, after the streaming step, and c is the x location of the particle two lattice nodes downstream, i.e., the particle starting $(x-2\sqrt{m_\sigma/m_\varsigma}\delta_t, y)$ for $\alpha=1$, after the streaming step. Interpolation schemes for directions $\alpha=1$–4 require distribution function values from three lattice nodes in order to determine the new value at each lattice node. For streaming directions $\alpha=5$–8, values from nine lattice nodes are necessary. The interpolation scheme is first done in one Cartesian direction, e.g., y, for three distribution functions, and then those values are used to calculate the distribution function at (x,y). Figure 1 shows the lattice setup corresponding to Eq. (28) for $\alpha=5$ with the following values for this model: $a-x=a'-y=\delta_x$, $x-b=y-b'=\sqrt{m_\sigma/m_\varsigma}\delta_x-\delta_x$, and $x-c=y-c'=2\sqrt{m_\sigma/m_\varsigma}\delta_x-\delta_x$. The square boxes represent the lattice nodes. The interpolation polynomial is first used to calculate the distribution function values at the solid circle locations. Then the value of the distribution function at the location of the solid square is determined from the distribution function values at the solid circles using the interpolation polynomial a second time.

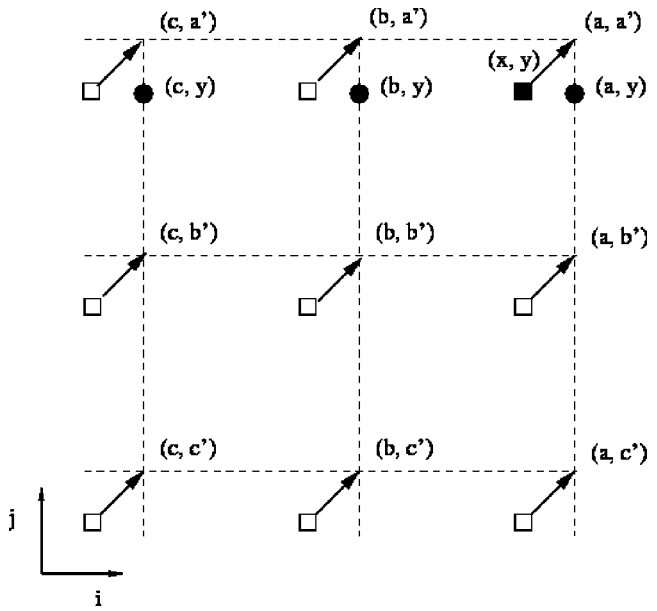

FIG. 1. Illustration of streaming and interpolation for species σ in the velocity direction $\alpha=5$ in a D2Q9 lattice model (squares represent lattice nodes).

The solution procedure for the DLS model is to first calculate the effects of collisions, then to stream the particle, and finally to use interpolation to determine the distribution function values at the lattice nodes. It is possible to combine the streaming and interpolation step.

One advantage of employing an interpolation scheme is that it can increase numerical stability. Another advantage is that interpolation reduces the resolution requirement of the LBM, thereby allowing for more efficient computations. However, as the distance $\sqrt{m_\sigma/m_\varsigma}\delta_x$ is increased, the accuracy of the interpolation decreases due to the increase in numerical diffusion. This limits the maximum ratio of molecular weights that can be simulated. From practical experience, it appears that in order to accurately capture the physics of binary diffusion, $m_\sigma/m_\varsigma \leqslant 9$ using this model.

It is also important to note that Lallemand and Luo [12] have shown some anisotropy effects to exist when using interpolation schemes [12]. Their work shows that when the equations are perturbed with a nonzero wave number the transport coefficients are anisotropic. However, zero-wave-number perturbations result in isotropic transport coefficients. The magnitude of these effects has not yet been tested for this interpolation scheme. Lallemand and Luo [12] have suggested using multiple relaxation time collision terms in order to mitigate this problem. A similar approach could be employed in this model.

IV. HYDRODYNAMIC EQUATIONS

It is of interest to determine the hydrodynamic equations associated with the lattice Boltzmann models proposed in Sec. II. This will allow us to determine the expression for the binary diffusion coefficient based upon the value of τ_D in Eq. (4). The Chapman-Enskog expansions for both the SLS and DLS models are similar. The main difference is that in the SLS model the lattice velocities, $\mathbf{e}_\alpha$, do not depend on the species. The expansions do not take into account the interpolation scheme employed in the numerical implementation of the DLS model during the streaming step. However, the interpolation scheme is second-order accurate, and the error associated with it should be similar to the overall order of the scheme.

Employing the expansions

$$f_\alpha^\sigma(\mathbf{x}+\mathbf{e}_\alpha\boldsymbol{\delta}_t,t+\boldsymbol{\delta}_t)=\sum_{n=0}\varepsilon^n(\partial_t+\mathbf{e}_\alpha^\sigma\cdot\nabla)^n f_\alpha^\sigma(\mathbf{x},t), \tag{29}$$

$$f_\alpha^\sigma=\sum_{n=0}\varepsilon^n f_\alpha^{\sigma(n)}, \tag{30}$$

$$\partial_t=\sum_{n=0}\varepsilon^n\partial_{t_n}, \tag{31}$$

in Eq. (2) (ignoring F_α^σ) yields the following relations for terms of order ε^1 and ε^2, respectively:

$$(\partial_{t_0}+\mathbf{e}_\alpha^\sigma\cdot\nabla)f_\alpha^{\sigma(0)}=-\frac{1}{\tau_\sigma}f_\alpha^{\sigma(1)}+J^{\sigma\varsigma}, \tag{32}$$

$$\partial_{t_1}f_\alpha^{\sigma(0)}+(\partial_{t_0}+\mathbf{e}_\alpha^\sigma\cdot\nabla)\left(1-\frac{1}{\tau_\sigma}\right)f_\alpha^{\sigma(1)}+\frac{1}{2}(\partial_{t_0}+\mathbf{e}_\alpha^\sigma\cdot\nabla)J^{\sigma\varsigma}=-\frac{1}{\tau_\sigma}f_\alpha^{\sigma(2)}. \tag{33}$$

The following moments of the distribution functions can be calculated for both models [4] (for the SLS model $\mathbf{e}_\alpha$ is not dependent on the species):

$$\sum_\alpha J_\alpha^{\sigma\varsigma}=0, \tag{34}$$

$$\sum_\alpha J_\alpha^{\sigma\varsigma}\mathbf{e}_\alpha^\sigma=-\frac{1}{\tau_D}\frac{\rho_\sigma\rho_\varsigma}{\rho\delta_t}(\mathbf{u}_\sigma-\mathbf{u}_\varsigma), \tag{35}$$

$$\sum_\alpha J_\alpha^{\sigma\varsigma}e_{\alpha i}^\sigma e_{\alpha j}^\sigma=-\frac{1}{\tau_D}\frac{\rho_\sigma\rho_\varsigma}{\rho\delta_t}\left((u_i\delta u_j+u_j\delta u_i)-\frac{1}{c_s^{\sigma 2}}u_iu_j\mathbf{u}\cdot\delta\mathbf{u}\right)\approx 0, \tag{36}$$

$$\sum_\alpha f_\alpha^{\sigma(0)}\mathbf{e}_{\alpha i}^\sigma\mathbf{e}_{\alpha j}^\sigma=c_s^{\sigma 2}\rho_\sigma\delta_{ij}+\rho_\sigma u_iu_j+\rho_\sigma\left((u_\sigma-u)_iu_j+(u_\sigma-u)_ju_i-\frac{u_iu_j\mathbf{u}\cdot(\mathbf{u}_\sigma-\mathbf{u})}{c_s^{\sigma 2}}\right), \tag{37}$$

$$\sum f_\alpha^{\sigma(0)}\mathbf{e}_{\alpha l}^\sigma\mathbf{e}_{\alpha j}^\sigma\mathbf{e}_{\alpha k}^\sigma=c_s^{\sigma 2}\rho_\sigma\Delta_{ijkl}u_l\left(1-\frac{\mathbf{u}\cdot(\mathbf{u}_\sigma-\mathbf{u})}{c_s^{\sigma 2}}\right)+c_s^{\sigma 2}\rho_\sigma\Delta_{ijkl}(u_\sigma-u)_l+\cdots, \tag{38}$$

where $\delta\mathbf{u}\equiv(\mathbf{u}_\sigma-\mathbf{u}_\varsigma)$, $\delta u_i\equiv(u_{\sigma i}-u_{\varsigma i})$, and

$$\Delta_{ijkl}=\delta_{ij}\delta_{kl}+\delta_{ik}\delta_{jl}+\delta_{il}\delta_{jk}. \tag{39}$$

The species mass conservation equations of first and second order in ε can be determined by summing Eqs. (32) and (33) over the velocity directions, α, which, respectively, yields

$$\partial_{t_0}\rho_\sigma+\nabla\cdot(\rho_\sigma\mathbf{u}_\sigma)=0, \text{ and} \tag{40}$$

$$\partial_{t_1}\rho_\sigma-\frac{1}{2}\nabla\cdot\left(\frac{1}{\tau_D}\frac{\rho_\sigma\rho_\varsigma}{\rho\delta_t}(\mathbf{u}_\sigma-\mathbf{u}_\varsigma)\right)=0, \tag{41}$$

where $\Sigma_\alpha f_\alpha^{\sigma(n)}=0$ for $n>0$. Adding Eq. (40) and ε times Eq. (41), and setting $\varepsilon=\delta_t$ gives the species mass conservation equation,

$$\partial_t\rho_\sigma+\nabla\cdot(\rho_\sigma\mathbf{u}_\sigma)=\frac{1}{2}\nabla\cdot\left(\frac{1}{\tau_D}\frac{\rho_\sigma\rho_\varsigma}{\rho}(\mathbf{u}_\sigma-\mathbf{u}_\varsigma)\right). \tag{42}$$

Combining Eq. (42) for each species yields the overall mass conservation,

$$\partial_t\rho+\nabla\cdot(\rho\mathbf{u})=0. \tag{43}$$

Now we want to find the relationship for the binary diffusion coefficient. Rearranging Eq. (42) gives

$$\partial_t\rho_\sigma+\nabla\cdot(\rho_\sigma\mathbf{u})=-\left(1-\frac{1}{2\tau_D}\right)\nabla\cdot\mathbf{j}_\sigma, \tag{44}$$

where

$$\mathbf{j}_\sigma=\rho_\sigma(\mathbf{u}_\sigma-\mathbf{u})=\frac{\rho_\sigma\rho_\varsigma}{\rho}(\mathbf{u}_\sigma-\mathbf{u}_\varsigma), \tag{45}$$

using the identity that $\rho(u_\sigma-u)=\rho_\varsigma(u_\sigma-u_\varsigma)$. Notice that in the right-hand side of Eq. (44) the premultiplication factor has an extra term, $1/2\tau_D$, which will result in a correction factor in the diffusion coefficient expression. In general, the mass flux vector, $\mathbf{j}_\sigma$, including ordinary and pressure diffusion effects is (Eq. (8.1-7) of [13])

$$\mathbf{j}_\sigma=-\frac{n^2}{\rho}m_\sigma m_\varsigma D_{\sigma\varsigma}\mathbf{d}_\sigma, \tag{46}$$

where the number density, $n=n_\sigma+n_\varsigma=\rho_\sigma/m_\sigma=\rho_\varsigma/m_\varsigma$. The diffusion force, $\mathbf{d}_\sigma$, has the property $\mathbf{d}_\sigma=-\mathbf{d}_\varsigma$ and the relationship

$$\mathbf{d}_\sigma=\nabla\left(\frac{n_\sigma}{n}\right)+\frac{n_\sigma n_\varsigma}{n\rho}(m_\varsigma-m_\sigma)\nabla\ln p. \tag{47}$$

Luo and Girimaji [4] have derived the following relationship for the diffusion force for this lattice Boltzmann model:

$$(\mathbf{u}_\sigma-\mathbf{u}_\varsigma)=-\tau_D\delta_t\frac{\rho p}{\rho_\sigma\rho_\varsigma}\mathbf{d}_\sigma. \tag{48}$$

Using Eq. (48) in Eq. (45), Eq. (44) can be rewritten as

$$\partial_t \rho_\sigma + \nabla \cdot (\rho_\sigma \mathbf{u}) = \left(1 - \frac{1}{2\tau_D}\right) \nabla \cdot (\tau_D \delta_t p \mathbf{d}_\sigma). \quad (49)$$

In order to get the correct species mass conservation equation for species σ, i.e.,

$$\partial_t \rho_\sigma + \nabla \cdot (\rho_\sigma \mathbf{u}) = \nabla \cdot \left(\frac{n^2 m_\sigma m_\varsigma}{\rho} D_{\sigma\varsigma} \mathbf{d}_\sigma\right), \quad (50)$$

which would have resulted from using Eq. (46) in Eq. (44) without the additional $1/2\tau_D$ term, the binary diffusion coefficient must have the relationship

$$D_{\sigma\varsigma} = \frac{\rho p}{n^2 m_\sigma m_\varsigma}\left(\tau_D - \frac{1}{2}\right)\delta_t. \quad (51)$$

Notice that in order to simulate the same binary diffusion coefficient at every location in a computational domain, τ_D will depend on the other parameters in Eq. (51).

Now we will derive the conservation of momentum equation associated with the SLS and DLS models. The Euler level conservation of momentum equation is found by summing $\mathbf{e}_\alpha^\sigma$ times Eq. (32) over the velocity directions, which in the incompressible limit gives

$$\partial_{t_0}(\rho_\sigma \mathbf{u}_\sigma) + (\rho_\sigma \mathbf{u}_\sigma \cdot \nabla)\mathbf{u} = -\nabla p_\sigma - \frac{1}{\tau_D \delta_t}\frac{\rho_\sigma \rho_\varsigma}{\rho}(\mathbf{u}_\sigma - \mathbf{u}_\varsigma), \quad (52)$$

where $p_\sigma = \rho_\sigma c_s^{\sigma 2}$. In this derivation, we use the argument that in general the diffusion velocities of the two species are small relative to the mass averaged velocity. We may then neglect terms of the order $(u_\sigma - u)_i u_j$ and $ui\delta u_i$. The second-order expansion in ε yields the conservation of momentum equation which is determined by summing $\mathbf{e}_\alpha^\sigma$ times Eq. (33) over the velocity directions, which yields

$$\partial_{t_1}(\rho_\sigma \mathbf{u}_\sigma) = \frac{1}{\delta_t} v_\sigma \nabla^2(\rho_\sigma \mathbf{u}_\sigma) - \frac{1}{2}\partial_{t_0}\left(\frac{1}{\tau_D}\frac{\rho_\sigma \rho_\varsigma}{\rho \delta_t}(\mathbf{u}_\sigma - \mathbf{u}_\varsigma)\right), \quad (53)$$

where the viscosity, v_σ, is

$$v_\sigma = c_s^{\sigma 2}\left(\tau_\sigma - \frac{1}{2}\right)\delta_t. \quad (54)$$

The last term in Eq. (53) can be evaluated by applying a chain rule and using Eqs. (40) and (42). However, we are interested in the mass averaged momentum equations. The momentum equation for each species is found by adding Eq. (52) to ε times Eq. (53) to yield

$$\partial_t(\rho_\sigma \mathbf{u}_\sigma) + (\rho_\sigma \mathbf{u}_\sigma \cdot \nabla)\mathbf{u} = -\nabla p_\sigma + v_\sigma \nabla^2(\rho_\sigma \mathbf{u}_\sigma) - \left(1 + \frac{\varepsilon}{2}\partial_{t_0}\right) \times \left(\frac{1}{\tau_D}\frac{\rho_\sigma \rho_\varsigma}{\rho \delta_t}(\mathbf{u}_\sigma - \mathbf{u}_\varsigma)\right). \quad (55)$$

The mass averaged momentum equation is found by adding together Eq. (55) for each species, which gives

$$\partial_t(\rho \mathbf{u}) + (\rho \mathbf{u} \cdot \nabla)\mathbf{u} = -\nabla p + v_\sigma \nabla^2(\rho_\sigma \mathbf{u}_\sigma) + v_\varsigma \nabla^2(\rho_\varsigma \mathbf{u}_\varsigma), \quad (56)$$

where $p = p_\sigma + p_\varsigma$.

V. BINARY DIFFUSION

In order to evaluate the DLS model, two sets of computations are carried out. The simpler case is that of two gases with the same properties diffusing into each other. For simulations of fluids with identical molecular weights, the DLS model is essentially identical to the SLS model. The results from calculations using the DLS LBM are compared to the solution obtained by applying Fick's law in the macroscopic limit. In this computation, the properties of nitrogen at 300 K and 1 bar are employed for both gases. The binary diffusion coefficient, $D_{\sigma\varsigma}$, is 0.68 cm^2/s which leads to a value of $\tau_D = 1.1$. The computational domain has 500 lattice nodes in the y direction with periodic boundary conditions on the horizontal boundaries and bounce-back boundary conditions on the vertical boundaries. The lattice parameters have the following values: $\delta_x = 3.85$ μm and $\delta_t = 44$ ns. The initial density profile for each species is assumed to have a hyperbolic tangent profile with the form

$$\rho_\sigma(y) = \frac{1}{2}\left[(\rho_{\sigma,h} + \rho_{\sigma,l}) + (\rho_{\sigma,h} - \rho_{\sigma,l})\tanh\left(\frac{y - \frac{1}{2}y_{\max}}{\delta_{th}}\right)\right], \quad (57)$$

$$\rho_\varsigma(y) = \frac{1}{2}\left[(\rho_{\varsigma,h} + \rho_{\varsigma,l}) + (\rho_{\varsigma,h} - \rho_{\varsigma,l})\tanh\left(\frac{y - \frac{1}{2}y_{\max}}{\delta_{th}}\right)\right], \quad (58)$$

where $y_{\max}$ is the domain length and δ_{th} is the thickness of the diffusion profile. For this computation, $\delta_{th} = 0.1$ mm. The minimum and maximum densities are $\rho_{\sigma,h} = \rho_{\varsigma,h} = 1.123$ kg/m^2 and $\rho_{\sigma,l} = \rho_{\varsigma,l} = 0.07$ kg/m^2.

The Fick's law computations are based upon a discretized form of the equation

$$\partial_t \rho_\sigma = -D_{\sigma\varsigma}\partial_{yy}\rho_\sigma. \quad (59)$$

The length of the domain is divided into 500 equally spaced nodes. Figure 2 shows the density profile of each species at $t = 0$, 0.044, 0.088, and 0.176 ms, for both the LBM and Fick's law computations. The results from Fick's law and the LBM model compare well with less than 1% error at all locations and times.

The second study is that of two gases with different molecular weights diffusing into each other. The properties of nitrogen at 273 K and 1 bar are employed for one gas, and the properties of helium at 273 K and 1 bar are employed for the other gas. The binary diffusivity is $D_{\sigma\varsigma} = 0.632$ cm^2/s. The corresponding value of τ_D at each location is calculated using Eq. (51). The computational domain has 500 lattice nodes in the y direction and boundary conditions are the same as in the previous study. The lattice spacing is $\sqrt{7}\delta_x$

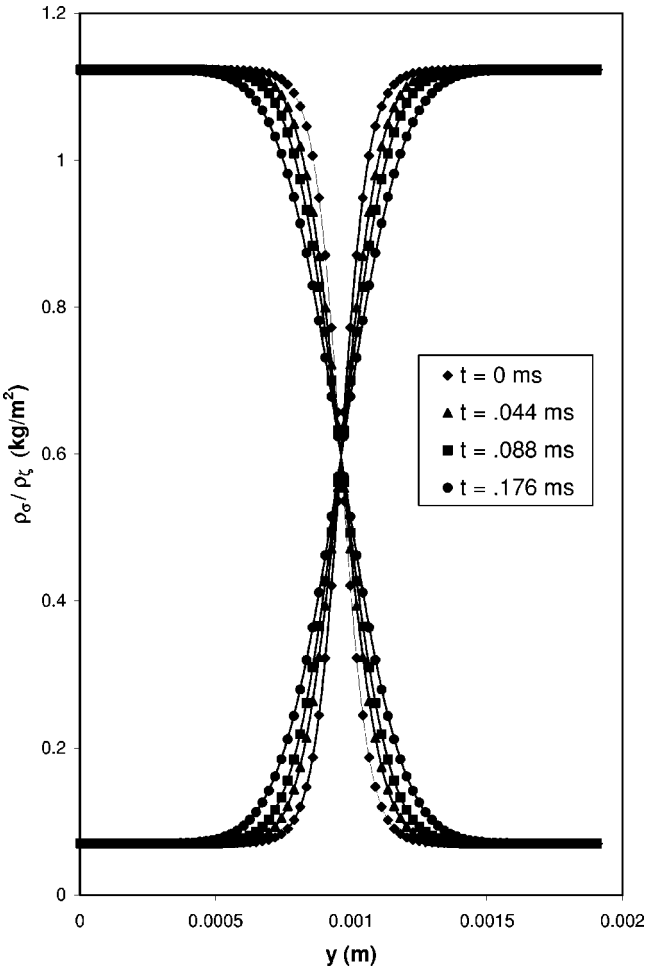

FIG. 2. Density profile for binary diffusion of two species with the same molecular weight at several times (solid lines - Fick's law, symbols–DLS LBM).

with $\delta_x = 2\ \mu$m and $\delta_t = 3$ ns. The initial gas density for each species follows Eqs. (57) and (58) with $\delta_{th} = 0.05$ mm, $\rho_{\sigma,h} = 1.250\ \mathrm{kg/m^2}$, $\rho_{\varsigma,h} = 1.123\ \mathrm{kg/m^2}$, $\rho_{\sigma,l} = 0.0007\ \mathrm{kg/m^2}$, and $\rho_{\varsigma,l} = 0.0001\ \mathrm{kg/m^2}$. The LBM results are compared to computations using a one-dimensional (1D) diffusion code, which solves the macroscopic species diffusion equation for multicomponent mixtures [14]. This code solves the transient multicomponent species equations for reacting mixtures. Here convection is not considered. Reactions are neglected. The equations are spatially discretized with a second-order central-difference scheme and temporally with a first-order scheme. Figure 3 illustrates the density profile for each species at $t = 0$, 0.02, 0.05, and 0.1 ms from both the LBM computations employing the DLS method and the 1D diffusion code computations. The two solutions compare well with a difference of less than 1% for all locations and times.

Now we compare the DLS and SLS models. As mentioned in Sec. II, the SLS model is not able to simulate fluids with molecular weight ratios greater than 3 when the speed of sound of the heavier species is given by $c_s^\sigma = 1/\sqrt{3}c$. Therefore, we simulate two gases with a molecular weight ratio of 2 diffusing into each other. As with the previous studies, the initial gas density for each species follows Eqs. (57) and (58)

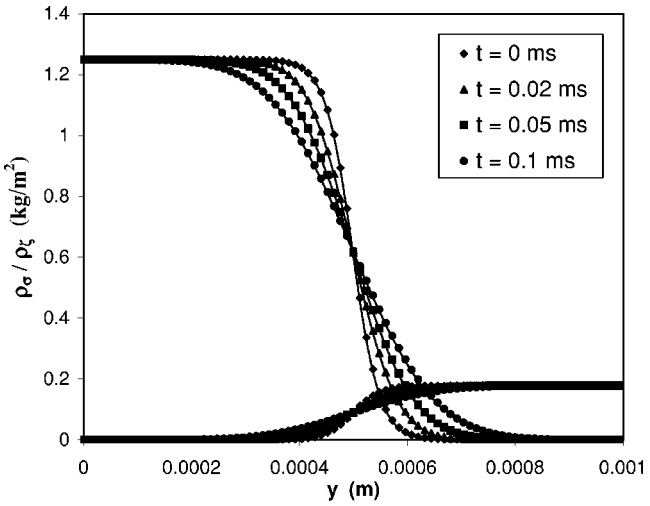

FIG. 3. Density profile for binary diffusion of two species with molecular weight ratio of 7/1 at several times (solid lines - diffusion code, symbols–DLS LBM).

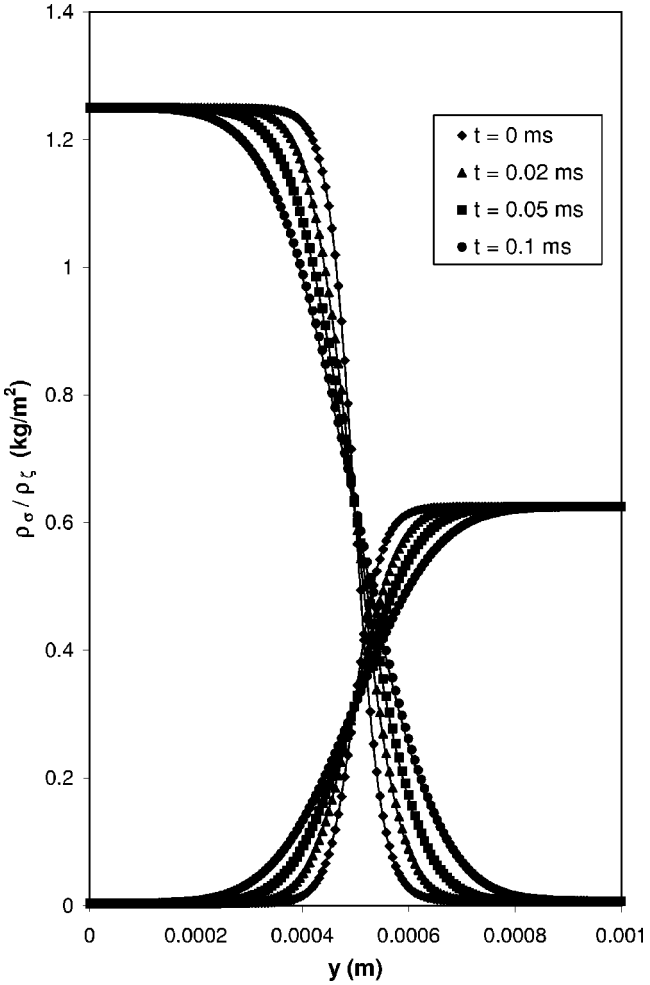

FIG. 4. Density profile for binary diffusion of two species with molecular weight ratio of 2/1 at several times (solid lines–DLS LBM, symbols–SLS LBM).

with $\delta_{th}=0.05$ mm, $\rho_{\sigma,h}=1.250$ kg/m^2, $\rho_{s,h}=0.625$ kg/m^2, $\rho_{\sigma,l}=0.0007$ kg/m^2, and $\rho_{s,l}=0.000\,35$ kg/m^2. The lattice spacing for the SLS model is δ_x with a total of 500 nodes in the y direction, while the lattice spacing for the DLS model is $\sqrt{2}\delta_x$ with 354 nodes in the y direction. For both models, $\delta_x=2$ μm, $\delta_t=3$ ns, and $D_{\sigma s}=0.632$ cm^2/s. Figure 4 shows the density profile for each species at $t = 0$, 0.02, 0.05, and 0.1 ms for both the DLS and SLS computations. Similar to the previous computations, the two solutions have a difference of less than 1%.

VI. DISCUSSION AND CONCLUSIONS

In this paper, we have proposed two lattice Boltzmann models for simulating diffusion of gases with different molecular weights based upon the general model of Luo and Girimaji [3,4]. The same lattice spacing (SLS) method employed the same streaming distance and time step for each fluid, but altered the equilibrium distribution function in order to simulate different speeds of sound. The different lattice spacing (DLS) method varied the streaming distance for each species, while maintaining the same time step. This approach is physically intuitive since lighter molecules move at larger velocities than heavier molecules. In this way, the speed of sound is naturally altered for each species and the equilibrium distribution function is consistent with kinetic theory. Both models were shown to reproduce the correct macroscopic hydrodynamic equations.

The models were tested on binary diffusion problems. The DLS method was employed to simulate self-diffusion and N_2-He diffusion. The results compared well with the solution of the macroscopic Fick's law for self-diffusion and the solution of the macroscopic, multicomponent species diffusion equations for N_2-He diffusion with differences of less than 1% in both cases. The SLS model was compared to the DLS model for computing binary diffusion between fluids with a ratio of molecular weights of 2. The difference between density profiles of the two methods was less than 1%.

The DLS model is deemed superior to the SLS model because it is able to simulate higher ratios of molecular weights for the same speed of sound. The DLS model also has a more rigorous physical basis. The use of interpolation limits the maximum attainable ratio of molecular weights for the DLS model, but the ratio is still greater than for the SLS model. The DLS model has been employed to conduct initial studies of transient mixing layers [15,16].

ACKNOWLEDGMENTS

The authors thank Dr. Kannan Premnath, Dr. Venkatesh Gopalakrishnan, and Dr. Li-Shi Luo for useful discussions during the course of this work. They thank Information Technologies at Purdue University.

[1] X. Shan and G. Doolen, J. Stat. Phys. **81**, 379 (1995).
[2] X. Shan and G. Doolen, Phys. Rev. E **54**, 3614 (1996).
[3] L.-S. Luo and S. S. Girimaji, Phys. Rev. E **66**, 035301(R) (2002).
[4] L.-S. Luo and S. S. Girimaji, Phys. Rev. E **67**, 036302 (2003).
[5] X. He, X. Shan, and G. Doolen, Phys. Rev. E **57**, R13 (1998).
[6] L.-S. Luo, Phys. Rev. E **62**, 4982 (2000).
[7] L. Sirovich, Phys. Fluids **5**, 908 (1962).
[8] E. Goldman and L. Sirovich, Phys. Fluids **10**, 1928 (1967).
[9] X. He and L.-S. Luo, Phys. Rev. E **55**, R6333 (1997).
[10] D. Wolf-Gladrow, *Lattice-Gas Cellular Automata and Lattice Boltzmann Models: An Introduction* (Springer, New York, 2000).
[11] X. He, L.-S. Luo, and M. Dembo, J. Comput. Phys. **129**, 357 (1996).
[12] P. Lallemand and L.-S. Luo, Phys. Rev. E **61**, 6546 (2000).
[13] J. Hirschfelder, C. Curtiss, and R. Bird, *Molecular Theory of Gases and Liquids* (Wiley, New York, 1954).
[14] V. Gopalakrishnan and J. Abraham, Combust. Flame **136**, 557 (2004).
[15] M. McCracken and J. Abraham, Int. J. Mod. Phys. C **16**, (2005).
[16] M. McCracken, Ph.D. thesis, Purdue University, West Lafayette, IN, 2004.